JOINT CONSTELLATION EXTENSION AND TONE RESERVATION FOR PAPR REDUCTION IN ADAPTIVE OFDM SYSTEMS

Mark Petermann, Dirk Wübben and Karl-Dirk Kammeyer

Department of Communications Engineering
University of Bremen
Otto-Hahn-Allee, 28359 Bremen, Germany
{petermann, wuebben, kammeyer}@ant.uni-bremen.de

ABSTRACT

One major drawback of Orthogonal Frequency Division Multiplexing (OFDM) is the large peak-to-average power-ratio (PAPR), which significantly degrades the power efficiency. In order to prevent nonlinear distortions the PAPR needs to be minimized to guarantee a linear dynamic range of the high power amplifier. Therefore, various reduction algorithms have been proposed. However, they do not include link adaptation requirements. Previous results show that bit and power loading algorithms in adaptive OFDM systems fail to meet the target error rate requirements if large time-domain peaks occur. Hence, in this paper a joint utilization of extended constellation alphabets of active subcarriers and tone reservation for peak power reduction in adaptive OFDM systems is derived. The resulting linear programming (LP) problem can be efficiently solved and the solution is lossless in terms of throughput. Furthermore, a suboptimal algorithm, which achieves great PAPR reduction with lower complexity, is proposed while link adaptation is employed.

1. INTRODUCTION

The advantage of Orthogonal Frequency Division Multiplexing (OFDM), namely an easy equalization of high rate data streams over frequency selective channels [1], comes along with the problem of a large peak-to-average power-ratio (PAPR) of the transmit time-domain signal [2]. This signal is distorted by the nonlinear characteristic of the high power amplifier (HPA) usually employed at the transmitter, which leads to a spectral regrowth. Several techniques were proposed to reduce this ratio, a good overview can be found in [3]. The simplest principle is (repeatedly) clipping the amplitude and apply filtering afterwards [4]. This procedure leads to in-band distortions, which result in a bit error rate (BER) degradation. Multiple signal respresentation approaches as partial transmit sequences (PTS) [5] or selective mapping (SLM) [6] do not degrade the BER performance but require excessive computation of Inverse Fast Fourier Transforms (IFFTs). In contrast, tone reservation (TR) and tone injection (TI) methods are efficient means in terms of complexity and BER requirements. TR utilizes a set of unused or reserved subcarriers for PAPR reduction. The task is to optimize the signal of non-data bearing subcarriers, while keeping the data subcarriers unchanged. Due to the orthogonality of the subcarriers no distortions are caused. TI methods use extended constellations to map data constellation points into equivalent points, thus altering the data bearing subcarriers. One subclass of TI is the so-called active constellation extension (ACE) method, which modifies outer constellation points only. Thereby, the minimum euclidean distance of PSK/QAM symbols is kept and a BER degradation is avoided. Even smaller BER values are achievable with this scheme [7]. The opposed approaches using different subcarriers motivate the effective combination of both TR and ACE technique for PAPR reduction utilizing all available subcarriers [8, 9].

Large PAPR values not only occur in single modulation alphabet multicarrier systems, but also in adaptive OFDM systems, where bit and power loading (BPL) is applied. Hence, the problem must be considered likewise as previous results showed a performance decrease of link adaptation algorithms as different modulation schemes are used for a certain output back-off (OBO) of the HPA [10]. For PAPR reduction in adaptive OFDM systems some proposals like in [11] suggest a redistribution of bit and power levels on each subcarrier until the PAPR is beneath a certain threshold. Unfortunately, a given power constraint or a low PAPR constraint cannot be fulfilled with such an approach. In this contribution the bit and power loading algorithms remain unaffected and a combination of ACE and TR for PAPR reduction is investigated. Therefore, the solution of a convex optimization problem of such an adaptive approach is derived and compared with a suboptimal but less complex algorithm.

The remainder of the paper is organized as follows. In Section 2 the OFDM system is described and the PAPR reduction is stated. Furthermore, the constellation extension and tone reservation techniques are reviewed and the convex optimization formulation is given. The solution of the optimization problem is derived in Section 3 and an extended gradient-project method is presented. Simulation results are shown in Section 4 and a conclusion is given in Section 5.

Throughout the paper we use the following notation: Capital boldface letters denote frequency-domain column vectors or general matrices and small boldface letters describe column and time-domain vectors. The conjugate and the transpose are denoted by $(\cdot)^*$ and $(\cdot)^T$. Furthermore, $\mathbf{0}_{\alpha\times\beta}, \mathbf{I}_{\alpha\times\beta}$ are the $\alpha\times\beta$ all zero and all ones matrices/vectors, respectively. $\|\cdot\|_\ell$ describes the ℓ-norm, $|\cdot|$ stands for the cardinality of a set or the absolute value, whereas sets are denoted by caligraphic letters.

2. SYSTEM DESCRIPTION

2.1. OFDM System and PAPR

In an OFDM system, where the bandwidth B is divided into N_c orthogonal subcarriers, the transmit baseband signal with N_u non-data bearing and $N_a = N_c - N_u$ data bearing subcarriers can be

This work was supported in part by the German Research Foundation (DFG) under grant Ka841-21/1.

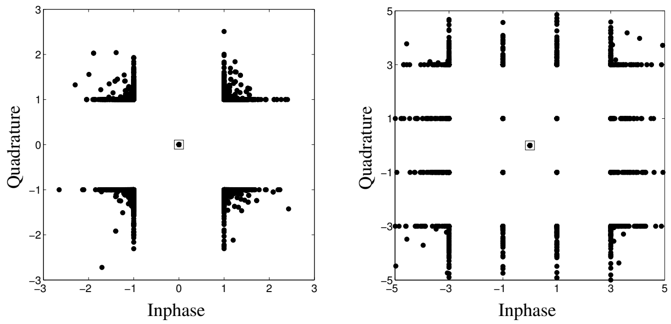

Fig. 1. Exemplary active constellation extension for QPSK (left) and 16-QAM (right) with zero symbols exploitable with TR techniques

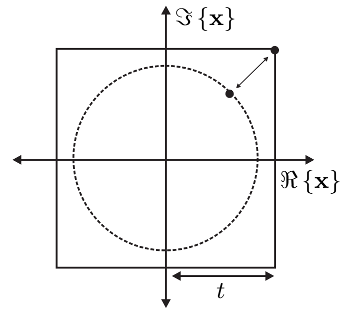

Fig. 2. Approximation of the power restricted complex envelope

obtained using the IFFT

$$x_n = \frac{1}{\sqrt{N_c}} \sum_{k=0}^{N_c-1} X_k \exp\left(j2\pi \frac{kn}{N_c}\right) \ , \tag{1}$$

for time index $n = 0, \dots, N_c - 1$, where X_k is the frequency-domain symbol of subcarrier k modulated using PSK/QAM with maximum modulation alphabet size $|\mathcal{M}|_{\max}$. For ease of notation we dropped the OFDM symbol index. Then, $\mathbf{x} = [x_0, \dots, x_{N_c-1}]^T$ is the time-domain symbol vector at the IFFT output, whose elements, due to the central limit theorem, can be modeled as truncated zero-mean Gaussian random variables. This leads to high peak values especially for an increasing number of subcarriers. Usually, an IFFT of a zero-padded input data vector of length wN_c is applied, where w is the oversampling factor. All peaks of the time-domain signal can be captured if an oversampling factor of $w \geq 4$ is used. Then, its corresponding discrete PAPR closely approximates that of the continuous-time signal. In this work all algorithms perform at Nyquist sampling rate, whereas the PAPR of the oversampled signal is measured. Consequently, the PAPR for such an OFDM system is defined as

$$\mathrm{PAPR}(\mathbf{x}) = \frac{\|\mathbf{x}\|_\infty^2}{\mathrm{E}\left\{\|\mathbf{x}\|_2^2\right\}/wN_c} \ , \tag{2}$$

where $\mathrm{E}\{\cdot\}$ denotes the expectation and $\|\mathbf{x}\|_\infty^2$ defines the peak value $\max_{\mathbf{x}} |x_k|^2$.

2.2. Convex Formulation

The PAPR defined in (2) can be significantly reduced, if the transmit signal $\mathbf{x}$ is modified by an additive time-domain signal $\mathbf{c} \in \mathbb{R}^{N_c \times 1}$, which is optimized with respect to ACE and TR constraints such that the corresponding PAPR

$$\mathrm{PAPR}(\mathbf{x}, \mathbf{c}) = \frac{\|\mathbf{x}+\mathbf{c}\|_\infty^2}{\mathrm{E}\left\{\|\mathbf{x}+\mathbf{c}\|_2^2\right\}/wN_c} \tag{3}$$

is minimized. The idea of ACE is shown in Fig. 1, where the constellation is extended on the outer points such that the minimum euclidean distance is not reduced. In the center of the depicted constellations some zeros are identifiable. These points correspond to the reserved/unused subcarriers. As there are no constellation restrictions for these subcarriers they can be used for TR techniques, meaning that these points can be extended in any direction without decreasing the bit error rate performance.

Following the principles in [2] and [12] the optimization problem using the ACE or/and TR technique can be written as

$$\underset{\mathbf{c}}{\text{minimize}} \, \|\mathbf{x}+\mathbf{c}\|_\infty = \underset{\mathbf{C}}{\text{minimize}} \, \|\mathbf{x}+\mathbf{FC}\|_\infty \ , \tag{4}$$

where $\mathbf{C}$ is the corresponding frequency-domain vector of the additive signal and $\mathbf{F}$ denotes the IDFT matrix of size $N_c \times N_c$ with elements $f_{n,k} = \left(1/\sqrt{N_c}\right)\exp\left(j2\pi kn/N_c\right)$. This convex problem can be interpreted as minimizing the squared magnitude of the resulting signal with respect to $\mathbf{c}$. Unfortunately, this is a minimization task in the complex plane, which results in a quadratically constraint quadratic program (QCQP) [8]. Such a problem is costly to solve. Hence, we transform this problem into a real-valued problem and optimize the magnitude of real and imaginary part independently. As real and imaginary part are dependent optimization variables, this leads to a suboptimal solution with a remaining small error.

Fig. 2 shows how this real-valued approach approximates the optimal solution circle of the power restricted complex envelope (dashed line), which depicts the maximum achievable peak power reduction resulting from the optimum complex optimization problem. The real-valued approach packs all time-domain samples in an outer square, where the maximum possible error is indicated by the two dots. The variable t will be explained in Sec. 3. The circle can be closer approximated by using additional phase-shifted versions of the time-domain signal block. This in turn escalates the amount of constraint equations especially in a link adaption scenario and slows down the convergence speed of the resulting algorithm [8]. This is a quite important aspect as the link adaption algorithms already introduce processing delays at the transmitter. Consequently, assume the real-valued system variables

$$\mathbf{X}_\mathrm{R} = \left[\Re\{\mathbf{X}\}\,\Im\{\mathbf{X}\}\right]^T \in \mathbb{R}^{2N_c \times 1} \tag{5a}$$

$$\mathbf{x}_\mathrm{R} = \left[\Re\{\mathbf{x}\}\,\Im\{\mathbf{x}\}\right]^T \in \mathbb{R}^{2N_c \times 1} \tag{5b}$$

$$\mathbf{C}_\mathrm{R} = \left[\Re\{\mathbf{C}\}\,\Im\{\mathbf{C}\}\right]^T \in \mathbb{R}^{2N_c \times 1} \tag{5c}$$

$$\mathbf{F}_\mathrm{R} = \begin{bmatrix} \Re\{\mathbf{F}\} & -\Im\{\mathbf{F}\} \\ \Im\{\mathbf{F}\} & \Re\{\mathbf{F}\} \end{bmatrix} \in \mathbb{R}^{2N_c \times 2N_c} \ , \tag{5d}$$

where $\mathbf{X}_\mathrm{R}$ is a real-valued ASK symbol vector with alphabet size $\sqrt{\mathcal{M}}$, $\mathbf{x}_\mathrm{R}$ the equivalent time-domain represenation, $\mathbf{C}_\mathrm{R}$ the frequency-domain correction term and $\mathbf{F}_\mathrm{R}$ the real-valued presentation of the IDFT matrix $\mathbf{F}$. Then, we can rewrite the optimization problem as

$$\underset{\mathbf{C}_\mathrm{R}}{\text{minimize}} \, \|\mathbf{x}_\mathrm{R} + \mathbf{F}_\mathrm{R}\mathbf{C}_\mathrm{R}\|_\infty \ , \tag{6}$$

which can now be written as a linear programming (LP) problem [2, 13].

3. JOINT OPTIMIZATION

3.1. Algorithm

The combination of ACE and TR introduces additional constraints to the optimization problem. For all N_u non-data bearing subcarriers there are no restrictions on the feasible region of the complex symbol after optimization. For all other N_a active carriers only those symbols corresponding to a corner or edge point of the selected complex symbol alphabet $\mathcal{M}$ are considered. In summary, this implies that only outer constellation symbols of the ASK signal $\mathbf{X}_{\mathrm{R}}$ are incorporated in the following optimization process of ACE. The beforehand determined set of ASK symbol indices used for optimization shall be indicated by $\mathcal{I}_c = \left[i_1, \ldots, i_{|\mathcal{I}_c|}\right]$. It is worth mentioning that the zero amplitude symbols of the non-data bearing subcarriers are also included in $\mathcal{I}_c$. Hence, by optimizing with respect to the constraints on $\mathcal{I}_c$ we jointly optimize the additive signal $\mathbf{c}$ including ACE and TR subcarriers. If we exclude the columns of the disregarded ASK symbols from the IDFT matrix such that $\tilde{\mathbf{F}}_{\mathrm{R}} = \left[\mathbf{f}_{i_1}, \mathbf{f}_{i_2}, \ldots, \mathbf{f}_{i_{|\mathcal{I}_c|}}\right] \in \mathbb{R}^{2N_c \times |\mathcal{I}_c|}$ and similarly arrange all frequency-domain correction symbols of the considered symbols in $\tilde{\mathbf{C}}_{\mathrm{R}} = \left[C_{i_1}, C_{i_2}, \ldots, C_{i_{|\mathcal{I}_c|}}\right]^T \in \mathbb{R}^{|\mathcal{I}_c| \times 1}$, then $\mathbf{F}_{\mathrm{R}}\mathbf{C}_{\mathrm{R}} = \tilde{\mathbf{F}}_{\mathrm{R}}\tilde{\mathbf{C}}_{\mathrm{R}}$ holds. If we then upperbound the objective function in (6) by a certain value t we can reformulate the optimization problem to

$$\text{minimize} \quad t \tag{7a}$$

$$\text{subject to} \quad \left| x_{\mathrm{R},k} + \mathbf{F}_{\mathrm{R}}^{(k)}\tilde{\mathbf{C}}_{\mathrm{R}} \right| \leq t \quad \forall\, k \in \mathcal{I}_c\ , \tag{7b}$$

where $\mathbf{F}_{\mathrm{R}}^{(k)}$ denotes the k-th row of matrix $\mathbf{F}_{\mathrm{R}}$. The element-wise inequality constraints for the absolute values in (7b) can be written in matrix form

$$\begin{bmatrix} \tilde{\mathbf{F}}_{\mathrm{R}} & \mathbf{I}_{2N_c \times 1} \\ -\tilde{\mathbf{F}}_{\mathrm{R}} & \mathbf{I}_{2N_c \times 1} \end{bmatrix} \begin{bmatrix} \tilde{\mathbf{C}}_{\mathrm{R}} \\ t \end{bmatrix} \geq \begin{bmatrix} -\mathbf{x}_{\mathrm{R}} \\ \mathbf{x}_{\mathrm{R}} \end{bmatrix}\ , \tag{8}$$

whereas the set limitation in (7b) can be stated with respect to the feasible regions of the transmit symbols

$$S_k C_{\mathrm{R},k} \geq 0 \quad \forall \quad k \in \mathcal{I}_c \tag{9a}$$

$$C_{\mathrm{R},k} \stackrel{!}{=} 0 \quad \forall \quad k \notin \mathcal{I}_c\ , \tag{9b}$$

where $S_k = \operatorname{sgn}\{X_{\mathrm{R},k}\} \in \{-1, 0, +1\}$ is the sign of the kth ASK symbol. The constraints of inner constellation points and the unconsidered real and imaginary parts of edge points of the QAM symbols are given in (9b). These constraints can be easily fulfilled if they are excluded from the optimization problem. The inequality constraints in (9a) can again be written in matrix form with element-wise inequality

$$\mathbf{S}\tilde{\mathbf{C}}_{\mathrm{R}} \geq \mathbf{0}_{|\mathcal{I}_c| \times 1}\ . \tag{10}$$

In (10) the sign variables are arranged in a diagonal matrix such that $\mathbf{S} = \operatorname{diag}\left\{S_1, \ldots, S_{|\mathcal{I}_c|}\right\}$. At last, by defining the auxiliary vectors $\mathbf{d} = \left[\mathbf{0}_{1 \times |\mathcal{I}_c|}\ 1\right]^T \in \mathbb{R}^{|\mathcal{I}_c|+1 \times 1}$ and $\mathbf{y}_{\mathrm{R}} = \left[\tilde{\mathbf{C}}_{\mathrm{R}}\ t\right]^T \in \mathbb{R}^{|\mathcal{I}_c|+1 \times 1}$ the optimization problem in (7) becomes

$$\text{minimize} \quad \mathbf{d}^T\mathbf{y}_{\mathrm{R}} \tag{11a}$$

$$\text{subject to} \quad \mathbf{A}_{\mathrm{R}}\mathbf{y}_{\mathrm{R}} \geq \mathbf{b}_{\mathrm{R}}\ , \tag{11b}$$

with matrix $\mathbf{A}_{\mathrm{R}}$ and vector $\mathbf{b}_{\mathrm{R}}$ given by

$$\mathbf{A}_{\mathrm{R}} = \begin{bmatrix} \tilde{\mathbf{F}}_{\mathrm{R}} & \mathbf{I}_{2N_c \times 1} \\ -\tilde{\mathbf{F}}_{\mathrm{R}} & \mathbf{I}_{2N_c \times 1} \\ \mathbf{S} & \mathbf{0}_{|\mathcal{I}_c| \times 1} \end{bmatrix} \quad \text{and} \quad \mathbf{b}_{\mathrm{R}} = \begin{bmatrix} -\mathbf{x}_{\mathrm{R}} \\ \mathbf{x}_{\mathrm{R}} \\ \mathbf{0}_{|\mathcal{I}_c| \times 1} \end{bmatrix}\ . \tag{12}$$

This is a LP problem [13] with $2N_c + 1$ variables and $4N_c + |I_c|$ constraints. The minimum solution value of t describes the size of the approximate square as shown in Fig. 2. In our investigations this LP was solved via the CVX toolbox [14] or the more efficient iterative Newton method in [15], which works considerably well with a large number of constraints. Motivated by the reduced effectiveness of ACE for higher order modulations [12], one may introduce a restriction of the maximum constellation size, for which the ACE procedure is applied. Then, the number of constraints can be further reduced with the drawback of a more suboptimal solution.

3.2. Extended Gradient-Project Approximation (EGPA)

One possible alternative method for approximating the previously described LP is using a gradient-project approach like in [12] for the ACE component of Sec. 3 and extend it with an update rule for the additive correction term related to unused subcarriers [16]. This combines the properties of both iterative schemes in a single procedure. Therefore, we propose the following algorithm:

1. For each OFDM symbol obtain the acceptable extension directions depending on the modulation alphabet of each subcarrier allocated by the link adaptation algorithm and store them together with the subcarriers indices of the non-data bearing subcarriers. The indices of non-data bearing carriers shall be enclosed in the set $\mathcal{I}_u$. Apply an IFFT to the transmit symbol vector $\mathbf{X}$. Set $i = 0$, where i is the iteration index.
2. Clip the resulting signal $\mathbf{x}^{(i)}$ to a certain magnitude threshold T to obtain the clipped signal $\bar{\mathbf{x}}$.
3. Compute the clipped signal portion

$$\mathbf{c}_{\mathrm{clip}} = \bar{\mathbf{x}} - \mathbf{x}^{(i)} \tag{13}$$

and apply an FFT to obtain the frequency-domain samples $\mathbf{C}_{\mathrm{clip}}$.

4. For the ACE part of this scheme keep only those components of $\mathbf{C}_{\mathrm{clip}}$, which belong to allowable extension directions of the active subcarrier constellations. Store all components of $\mathbf{C}_{\mathrm{clip}}$, which belong to non-data bearing subcarriers, into $\mathbf{C}_{\mathrm{asus}}$ such that the elements are

$$C_{\mathrm{asus},k} = \begin{cases} C_{\mathrm{clip},k} & k \in \mathcal{I}_u \\ 0 & \text{else} \end{cases}\ . \tag{14}$$

Set the components of $\mathbf{C}_{\mathrm{TR}}$ in $\mathbf{C}_{\mathrm{clip}}$ and all remaining parts of $\mathbf{C}_{\mathrm{clip}}$ to zero.

5. Obtain the time-domain signals $\mathbf{c}_{\mathrm{TR}}$ and $\mathbf{c}$ by the IFFT of $\mathbf{C}_{\mathrm{TR}}$ and $\mathbf{C}_{\mathrm{clip}}$, respectively.
6. Determine a smart gradient step size μ and compute the updated time-domain signal

$$\mathbf{x}^{(i+1)} = \mathbf{x}^{(i)} + \mu\mathbf{c}_{\mathrm{ACE}} - \nu\mathbf{c}_{\mathrm{TR}}. \tag{15}$$

Here, the gradient step size μ is chosen as suggested for the smart gradient method in [12]. The factor ν ($\nu = \sqrt{N_C/N_u}$ in this paper) may also be optimized [16].

7. If a desired PAR reduction is achieved or a maximum iteration number $i_{\max}$ is reached, stop. Otherwise set $i = i + 1$ and goto 2).

It is worth mentioning that this algorithm introduces additional IFFT and FFT operations, which in turn slightly increases the complexity compared to the original OFDM system. For high spectral efficiencies all subcarriers are data bearing subcarriers especially if a maximum modulation alphabet size is set. Then this algorithm inherently reduces to the one in [12].

4. SIMULATION RESULTS

The performance of the described schemes is compared in this section. The adaptive, uncoded single-antenna OFDM system with an exemplary bandwidth of $B = 5$ MHz was simulated with $N_c = 256$ subcarriers. In addition, the number of non-data bearing subcarriers is determined by a bit and power loading algorithm, whose maximum allowed modulation alphabet size was set to $|\mathcal{M}|_{\max} = 256$ (QAM). Here, we restrict ourselves to the loading algorithm of Krongold [17]. It is worth mentioning that several other loading algorithms were proposed, which allow for utilization of our approach especially in coded scenarios [18, 19]. Depending on a predefined spectral efficiency η a total number of bits can be allocated to the subcarriers. For the BER analysis the frequency-domain channel coefficients $H_k \in \mathbb{C}$ result from the frequency-selective time-domain channel coefficients $h(\ell)$, $0 \le \ell \le L-1$, whose elements are i.i.d. complex Gaussian distributed according to $\mathcal{N}_C(0, 1/L)$. L denotes the number of uncorrelated equal power channel taps, where $L=6$ is used. Hence, the frequency-domain channel coefficients are obtained via

$$H_k = \frac{1}{L}\sum_{\ell=0}^{L-1} h(\ell)\, \mathrm{e}^{-j\Omega_k \ell}\,, \tag{16}$$

where $\Omega_k = 2\pi n/N_C$, $0 \le k \le N_C - 1$ are the equidistant sampling frequencies. H_k is known at the transmitter and is assumed to be constant over one OFDM symbol. A sufficiently long cyclic prefix of length 8 is selected.

Furthermore, the power of the noise on all subcarriers is fixed to $\sigma_n^2 = 1$. Hence, the signal-to-noise ratio is exclusively defined by the total available transmit power P. This total power is distributed according to the bit and power loading algorithm, where no power may be assigned to "bad" subcarriers. If these subcarriers are later on used for TR techniques, then the available powers of the active subcarriers are rescaled by $(N_c - N_u)/N_c$ and thus the remaining available transmit power $(1 - (N_c - N_u)/N_c) \cdot P$ is equally distributed among the previously free subcarriers. The oversampling factor is $w = 4$ and an amplifier is employed in the simulation chain as this device has a direct impact on the BER and the spectral leakage due to clipping effects. The well-known Rapp model as in [20] with parameter $p = 2$ and an input back-off (IBO) of 3 dB was applied.

In Fig. 3 the complementary cumulative distribution function (CCDF) of the PAPR is shown. There, the curves indicate the probability that the PAPR of one OFDM symbol exceeds a certain threshold, i.e.,

$$\mathrm{CCDF}\,(\mathrm{PAPR}\,(\mathbf{x}, \mathbf{c})) = Pr\,(\mathrm{PAPR}\,(\mathbf{x}, \mathbf{c}) > \gamma)\ , \tag{17}$$

where $Pr\,(\cdot)$ denotes probability and γ is the threshold in dB. The PAPR values are calculated according to (3). For the gradient-project method the clipping ratio was fixed to 3 dB and the maximum iteration number was either $i_{\max} = 3$ or $i_{\max} = 9$. Results are shown for a spectral efficiency of $\eta = 2$ bit/s/Hz. As can be seen from the CCDF results a PAPR reduction of around 2 dB is achieved with the joint ACE and TR technique if the square approximation is used. The gradient-project method with 3 iterations is able to achieve almost a similar behavior with a gap less than 0.7 dB compared to the LP solution. Further iterations are not justified as the performace gain of around 0.2 is negligible compared to the increased number of IFFT/FFT computations.

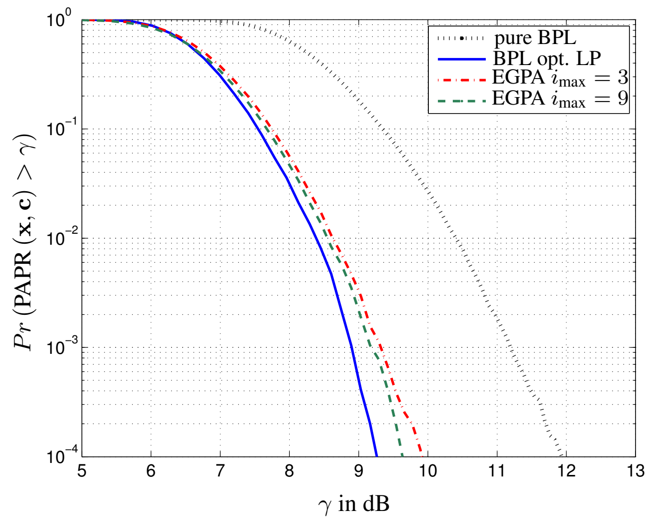

Fig. 3. PAPR CCDFs of different schemes with $N_c = 256$ subcarriers and a spectral efficiency of $\eta = 2$ bit/s/Hz

Regarding the uncoded BER performance incorporating the HPA in Fig. 4 a performance gain of the joint ACE/TR technique is obtained due to the reduced amount of samples, which are influenced by the nonlinear region of the HPA and due to the performance gain of ACE coming from the increased euclidean distance of some outer constellation symbols [7]. The small power loss stemming from the exploitation of previously unused carriers was compensated such that a gain of approx. 4 dB at 10^{-3} BER is visible. The results for the EGPA are comparable to the BER performance of the OFDM system without PAPR reduction. A small gain is obtained in the high SNR region, but no performance reduction occurs, which corresponds to the idea of ACE and TR. Even for the BER performance the amount of EGPA iterations can be kept small as no significant increase is apparent.

Concluding the comparison, the normalized average power spectral density (PSD) is shown in Fig. 5. It can be seen that the proposed schemes are also able to decrease the out-of-band radiation up to 2.5 dB compared to the original OFDM-BPL spectral mask, where the LP solution still is superior to the EGPA algorithm, but with marginal differences. Hence, the gradient-project algorithm is especially suited for suppression of out-of-band components.

5. CONCLUSION

In this paper, we derived a joint optimization formulation of ACE and TR, which can be efficiently solved as a LP problem using Newton methods. To avoid large processing delays in combination with bit and power loading algorithms suboptimal solutions are preferred. Therefore, the number of constraints was limited for the PAPR reduction in the complex baseband case. An extended gradient-project method combining ACE and TR in an iterative procedure was introduced, which shows quite good performance at moderate complexity.

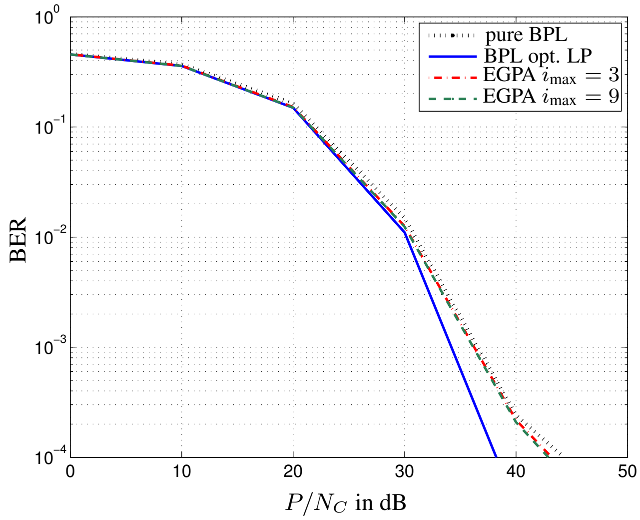

Fig. 4. Bit Error Rates with Tx power amplifier for different schemes and a spectral efficiency of $\eta = 2$ bit/s/Hz

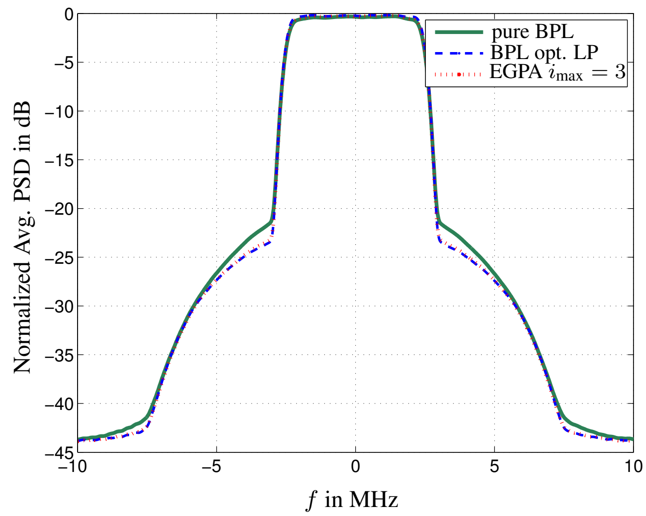

Fig. 5. Normalized Average Power Density Spectrum of OFDM Signals with Bit and Power Loading at bandwidth $B = 5$ MHz

6. REFERENCES

[1] J. A. C. Bingham, "Multicarrier modulation for data transmission: An idea whose time has come," *IEEE Commun. Mag.*, vol. 28, pp. 5–14, May 1990.

[2] J. Tellado, *Peak to Average Power Reduction for Multicarrier Communications Systems*, Ph.D. thesis, Stanford University, CA, USA, 2000.

[3] S. H. Han and J. H. Lee, "An overview of peak-to-average power ratio reduction techniques for multicarrier transmission," *IEEE Wireless Commun. Mag.*, vol. 12, no. 2, pp. 56–65, Apr. 2005.

[4] J. Armstrong, "New OFDM peak-to-average power reduction scheme," in *IEEE Proc. Vehicular Technology Conference (VTC) Spring*, Rhodes, Greece, May 2001.

[5] S. H. Müller and J. B. Huber, "OFDM with reduced peak-to-average power ratio by optimum combination of partial transmit sequences," *IEE Electronics Letters*, vol. 33, no. 5, pp. 368–369, Feb. 1997.

[6] R. Bäuml, R. F. H. Fischer, and J. B. Huber, "Reducing the peak-to-average power ratio of multicarrier modulation by selected mapping," *IEE Electronics Letters*, vol. 32, no. 22, pp. 2056–2057, Oct. 1996.

[7] T. F. Detwiler and D. L. Jones, "OFDM receiver design for active constellation extension," in *Proc. Asilomar Conference on Signals, Systems and Computers*, Monterey, CA, USA, Nov. 2005.

[8] B. S. Krongold and D. L. Jones, "An active-set approach for OFDM PAR reduction via tone reservation," *IEEE Trans. Signal Process.*, vol. 52, no. 2, pp. 495–509, Feb. 2004.

[9] Y. J. Kou, W.-S. Lu, and A. Antoniou, "New peak-to-average power-ratio reduction algorithms for multicarrier communications," *IEEE Trans. Circuits Syst. I*, vol. 51, no. 9, pp. 1790–1800, Sept. 2004.

[10] S. S. Das, F. Tariq, M. I. Rahman, F. B. Frederiksen, E. De Carvalho, and R. Prasad, "Impact of nonlinear power amplifier on link adaptation algorithm of OFDM systems," in *IEEE Proc. Vehicular Technology Conference (VTC) Fall*, Baltimore, MD, USA, Oct. 2007.

[11] Y. Chen, Y. Lee, and S. Lee, "PAPR reduction method using bit reallocation," U.S. Patent No. 7,313,195 B2, Dec. 2007.

[12] B. S. Krongold and D. L. Jones, "PAR reduction in OFDM via active constellation extension," *IEEE Trans. Broadcast.*, vol. 3, pp. 258–268, Sept. 2003.

[13] S. P. Boyd and L. Vandenberghe, *Convex Optimization*, Cambridge University Press, 2004.

[14] M. Grant and S. Boyd, "CVX: Matlab software for disciplined convex programming (web page and software)," `http://stanford.edu/~boyd/cvx`, Aug. 2008.

[15] O. L. Mangasarian, "A Newton method for linear programming," *Journal of Optimization Theory and Applications*, vol. 121, no. 1, pp. 1–18, Apr. 2004.

[16] H. Schmidt and K.-D. Kammeyer, "Reducing the peak to average power ratio of multicarrier signals by adaptive subcarrier selection," in *IEEE Int. Conf. Universal Personal Comm. (ICUPC)*, Florence, Italy, Oct. 1998, vol. 2.

[17] B. S. Krongold, K. Ramchandran, and D. L. Jones, "Computationally efficient optimal power allocation algorithms for multicarrier communication systems," *IEEE Trans. Commun.*, vol. 48, pp. 23–27, Jan. 2000.

[18] R. F. H. Fischer and J. B. Huber, "A new loading algorithm for discrete multitone transmission," in *IEEE Proc. Global Communications Conference (GLOBECOM)*, London, UK, Nov. 1996, pp. 724–728.

[19] C. Bockelmann, D. Wübben, and K.-D. Kammeyer, "Efficient coded bit and power loading for BICM-OFDM," in *IEEE Proc. Vehicular Technology Conference (VTC) Spring*, Barcelona, Spain, Apr. 2009.

[20] C. Rapp, "Effects of HPA-nonlinearity on a 4-DPSK/OFDM-signal for a digital sound broadcasting signal," in *Second European Conference on Satellite Communications (ECSC-2)*, Luettich, Belgium, Oct. 1991.